INFLUENCE OF Cu/Sn RATIO ON THE STRUCTURAL, MICROSTRUCTURAL AND OPTICAL PROPERTIES OF SPRAY DEPOSITED Cu$_2$SnS$_3$ THIN FILMS

U. CHALAPATHI[*], B. POORNAPRAKASH, S. H. PARK
Department of Electronic Engineering, Yeungnam University, 280 Daehak-ro, Gyeongsan-si,Gyeongsangbuk-do, South Korea,

Cu$_2$SnS$_3$ (CTS) thin films have been prepared by spray pyrolysis followed by annealing. The influence of Cu/Sn ratio on the structural, microstructural and optical properties of these films is investigated using appropriate characterization techniques. Energy dispersive X-ray spectroscopy analysis showed that the Cu/Sn ratio of these films is found to vary from 1.82 to 2.27. X-ray diffraction analysis of these films deposited with different Cu/Sn ratio are found to be monoclinic CTS with (-131)/(200) preferred orientation. Crystallite size of these films increased from 30 nm to be 35 nm with increasing the Cu/Sn ratio. Raman spectroscopy analysis of the Cu-correct CTS film showed the dominant modes due to monoclinic CTS phase. The grain size of these films was found to increase on increasing the Cu/Sn ratio. The direct optical band gap of these films is found to decrease from 0.99 eV to 0.90 eV with increasing the Cu/Sn ratio from 1.82 to 2.27.

1. Introduction

In recent years, Cu$_2$SnS$_3$ (CTS) is being explored as a promising material for thin film solar cells due to its suitable optical and electrical properties such as a direct optical band gap in the range 0.92−1.35 eV, absorption co-efficient (α) $> 10^4$ cm^{-1} and p-type electrical conductivity. In addition, the abundant and non-toxic elements present in this material made it as an alternative to CIGS, whose solar cells reached a maximum conversion efficiency of 21.7% [1] at the laboratory level but suffered to get large scale production due to the presence of scarce and expensive elements. CTS thin films were first prepared by Kuku and Fakolujo [2] by thermal evaporation. Several attempts have been made to growth CTS thin films using different techniques like evaporation [3, 4, 5, 6], sputtering [7], sulfurization of Cu, Sn precursor layers deposited by thermal evaporation [8, 9, 10], electron beam evaporation [11, 12, 13] sputtering [14, 15], electrodeposition [16, 17], and chemical methods like spray pyrolysis [18, 19], SILAR [20], spin coating [21], dip coating [22] etc. Among them, spray pyrolysis is simple and low-cost technique appropriate for the deposition of CTS thin films and understand their properties.

Studies on the growth and properties of spray deposited CTS thin films is quite meagre [18, 19, 23]. Adelifard et al. [18] prepared CTS films using a simple spray pyrolysis technique. The effect of Sn/Cu ratio (0.0 to 1.0) on the growth of CTS films was investigated. The films prepared from solutions with no Sn-salt exhibited covellite phase and with increased Sn/Cu ratio exhibited triclinic CTS phase. The direct band gap of these films decreased from 2.57 eV to 1.58 eV with increase in Sn/Cu molar ratio from 0.0 to 1.0. In our previous report [19], we also reported the growth of CTS films by spray pyrolysis and studied the annealing temperature effect on the growth of these films. CTS films annealed at 500 $^{\circ}$C exhibited monoclinic structure while the as-deposited films and films annealed at lower temperatures exhibited tetragonal structure. Tetragonal CTS films exhibited a band gap of ~1.10 eV and monoclinic CTS films exhibited a band gap of

_____
*Corresponding author: chalam.uppala@gmail.com

0.97 eV. Jia et al. [23] studied the influence of Cu precursor concentration and substrate temperature on the properties of spray deposited CTS films. They showed that CTS film deposited at 350 ^{o}C with 0.02 M Cu concentration has an atomic ratio of $Cu_{1.43}SnS_{2.59}$, and exhibited tetragonal structure with (112) preferential orientation. The film exhibited a direct optical band gap of 1.16 eV and electrical resistivity of 0.12 Ω-cm. In the present investigation, we have attempted to deposit CTS thin films using spray pyrolysis technique by varying the Cu salt concentration in the starting solution followed by annealing these films under sulfur atmosphere. The effect of Cu/Sn ratio on the growth and properties of these films is studied and the results are presented below.

2. Experimental details

The starting solution for the growth of Cu_2SnS_3 films consists of analar grade cupric chloride (0.018 M, 0.02 M and 0.022 M), stannic chloride (0.01 M) and thiourea (0.12 M) dissolved in distilled water. The three different Cu salt concentrations were used to obtain Cu-poor, Cu-correct and Cu-rich CTS films. These aqueous solutions containing different Cu salt concentrations were sprayed onto soda-lime glass substrates held at 360 ^{o}C using a pneumatically controlled air atomizing spray nozzle. The spray rate of the solution was kept at 12 ml/min. To improve the crystallization and reduce the sulfur deficiency in the films, these films were subjected to annealing under sulfur atmosphere in a two-zone tubular quartz furnace. Sulfur pellets were used as the sulfur source and nitrogen was used as the carrier gas. The samples temperature was increased at the rate of 20 ^{o}C/min up to 500 ^{o}C, while the sulfur source temperature was increased at the rate of 10 ^{o}C/min to 130 ^{o}C. The pressure in the tube during annealing was maintained at 1 mbar. These films were annealed at 500 ^{o}C for 60 min duration. After the annealing process, the sample temperature was slowly decreased at a rate of 5 ^{o}C/min up to 250 ^{o}C and was allowed to cool naturally to room temperature.

The crystal structure of these films is analysed by recording the X-ray diffraction (XRD) patterns using PANalytical X-ray diffractometer in the 2θ range 10-60° with CuKα radiation (λ = 0.15406 nm). Raman spectrum for the Cu-correct sample was recorded using Horiba Jobin Yvon HR 800UV micro Rama spectrometer coupled with confocal microscope. Surface morphology and elemental analysis were obtained using scanning electron microscope (SEM) attached with an energy dispersive X-ray spectroscopy (EDS). Spectral transmittance of the films was recorded with Cary 5000 UV-Vis-NIR double beam spectrophotometer in the wavelength range 300−2500 nm.

3. Results and discussion

3.1. Composition
The elemental compositions of the CTS films obtained by annealing the spray deposited films with three different Cu salt concentrations are shown in Table 1. The error in the determination of composition by EDS is ±5 at%. The Cu/Sn ratio is found to be 1.82 and S/(Cu+Sn) ratio is found to be 1.13 for the films deposited with 0.018 M Cu concentration and annealed at 500 0 C for an hour. The Cu/Sn ratio is found to increased from 2.03 to 2.27 and S/(Cu+Sn) ratio is found decreased from 1.09 to 1.03 on increasing the Cu salt concentration in the starting solution from 0.02 M to 0.022 M and annealing at 500 ^{o}C for an hour under sulfur atmosphere. Thus, the elemental composition of these films deposited with three different Cu salt concentrations in the solution followed by annealing is found to be Cu-poor, stoichiometric and Cu-rich CTS considering the accuracy limits of EDS analysis.

Table 1: Elemental composition of CTS films obtained by annealing the spray deposited
films with three different Cu salt concentrations in the solution

S.No.	Cu concentration (M)	Atomic percent			Ratio	
		Cu	Sn	S	Cu/Sn	S/(Cu+Sn)
1	0.018	30.29	16.63	53.09	1.82	1.13
2	0.020	32.06	15.76	52.18	2.03	1.09
3	0.022	34.21	15.05	50.74	2.27	1.03

3.2. Structural analysis

Fig. 1 shows the X-ray diffraction patterns of Cu-rich, stoichiometric and Cu-poor CTS films obtained by annealing the spray deposited films. The diffraction patterns of these films are found to exhibit an intense diffraction peak at 28.37^o followed by three week peaks at 32.89^o, 47.23^o and 56.08^o. These observed diffraction peaks are close to the cubic (JCPDS card no. 89-2877), monoclinic (JCPDS card no. 04-010-5719) and triclinic (JCPDS card no. 27-0198) CTS structures. Cubic CTS was reported to be a high temperature polymorphic [16], while triclinic CTS diffraction pattern has different normalized peak intensities than the observed peak intensities [19], hence they are unlikely in the present study. Thus, these observed diffraction peaks are attributed to monoclinic CTS phase. The intensity of XRD peaks increases and full width at half maximum (FWHM) of the peaks decrease by increasing the Cu/Sn ratio indicating an increase in the crystallite size of these films. The crystallite size, estimated from Scherrer's formula, is found to increase from 30 nm to 35 nm with increasing the Cu/Sn ratio from 1.82 to 2.27.
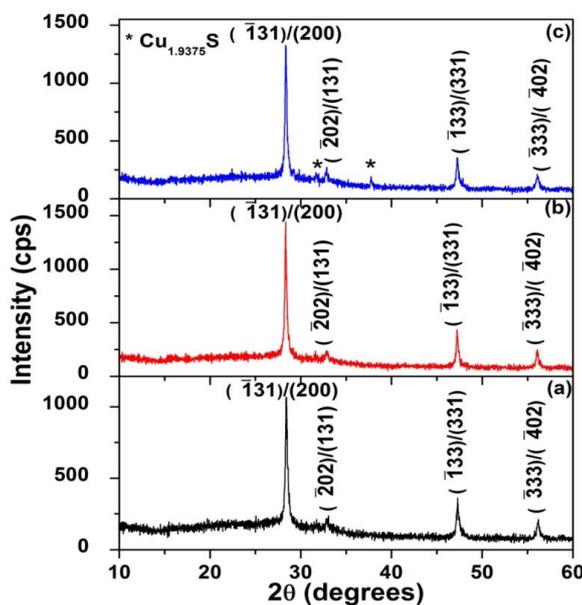
Fig. 1: XRD patterns of CTS films obtained with Cu/Sn ratios of (a) 1.82, (b) 2.03 and (C) 2.27.

We have carried out Raman spectroscopy analysis for Cu-correct samples to distinguish the possible secondary phases in these films. Fig. 2 shows the micro-Raman spectrum of CTS films obtained by annealing the spray deposited films. The Raman modes appear at 250 cm^{-1}, 290 cm^{-1}, 330 cm^{-1} and 348 cm^{-1} and 337 cm^{-1}. The observed intense Raman modes at 290 cm^{-1} and 348 cm^{-1} are matches with the reported Raman modes of monoclinic CTS phase [24] indicating the presence of dominant monoclinic CTS phase in these films. A week peak observed at 330 cm^{-1} is close to the reported intense Raman mode of tetragonal CTS phase [14]. A small hump observed

at 250 cm^{-1} is not close to any of the reported Raman 6modes of possible secondary phases and hence we are attributing this mode to monoclinic CTS phase since it is the dominant mode. Thus, the films deposited with Cu/Sn ratio of 2.03 shows the modes due to monoclinic CTS phase with a minor tetragonal CTS phase due to polymorphic nature of CTS.
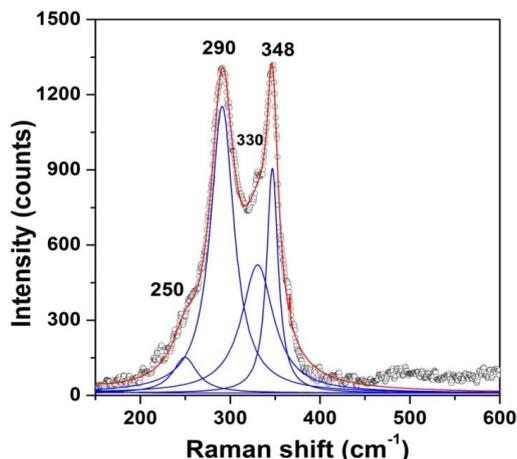
Fig. 2: Raman spectrum of Cu-correct CTS film obtained by annealing the spray deposited films

3.3. Microstructure

Fig. 3 shows the scanning electron microscopy (SEM) images of the CTS films obtained by annealing spray deposited films with different Cu salt concentrations. The microstructure of the Cu-poor CTS film (Fig. 3(a)) contains needle like crystals with an average grain size of 2 μm and smeary region. The smeary region decrease to a greater extent and grain size also improved in the case of films deposited with Cu/Sn = 2.03. For the films deposited with Cu/Sn = 2.27, there is a further increase in the grain size. The improved grain size is due to the improved Cu content in the films.
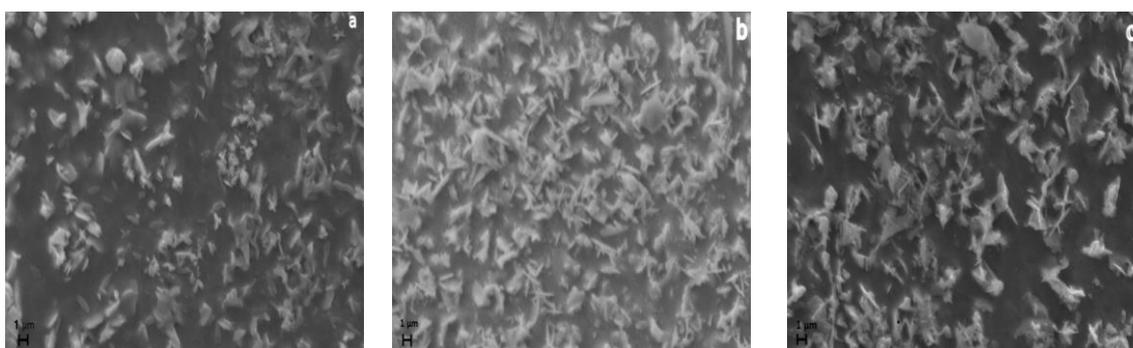
Fig. 3: SEM images of of annealed CTS films obtained with Cu/Sn
ratios of (a) 1.82, (b) 2.03 and (C) 2.27

3.4. Optical absorption

Fig. 4 shows the $(\alpha h v)^2$ versus hv plots of the CTS films obtained from their spectral transmittance data. The direct optical band gap of these films is found to decrease from 0.99 eV to 0.90 eV with increasing the Cu/Sn ratio from 1.82 to 2.27 in these films. The direct band gap values of monoclinic CTS phase was reported to be 0.93 eV by Berg et al. [16]. The obtained slightly different band gap values than the reported value might be due to the difference in the composition and crystallinity of the films.
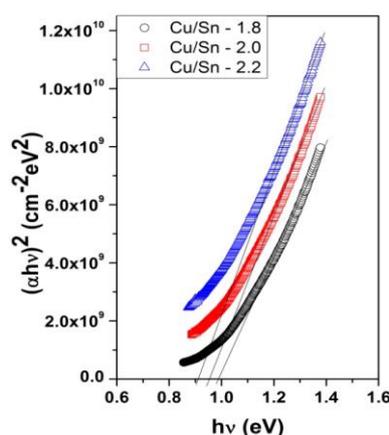
*Fig. 4: (αhv)^2 versus hv plots of CTS films obtained with different Cu/Sn ratio
by annealing the spray deposited films.*

4. Conclusions

In conclusion, CTS thin films are prepared by spray deposition followed by annealing in sulfur atmosphere. The effect of Cu/Sn ratio on the structural, microstructural and optical properties of CTS films is investigated. The films are found to be monoclinic CTS with (131)/(200) preferred orientation. CuS is observed as a secondary phase in the films growth with Cu-rich composition. The grain size of the films is found to increase with increase in the Cu/Sn ratio. The direct optical band gap of these films is found to decrease from 0.99 eV to 0.90 eV with increasing the Cu/Sn ratio.

References

[1] P. Jackson, D. Hariskos, R. Wuerz, O. Kiowski, A. Bauer, T. M. Friedlmeier, M. Powalla, Phys. Status Solidi (RRL) **9999**, 28 (2014).
[2] T. A. Kuku, O. A. Fakolujo, Sol. Energy Mater. **16**, 199 (1987).
[3] U. Chalapathi, Y. Jayasree, S. Uthanna, V. Sundara Raja, Vacuum **117**, 121 (2015).
[4] V. Robles, J. Trigo, C. Guill′en, J. Herrero, J. Alloy. Compd. 642 (2015) 40–44.
[5] A. Kanai, K. Toyonaga, K. Chino, H. Katagiri, H. Araki, Jap. J. Appl. Phys. **54,** 08KC06 (2015).
[6] T. S. Reddy, R. Amiruddin, M. S. Kumar, Sol. Energy Mater. Sol. Cells **143**, 128 (2015).
[7] M. Umehara, Y. Takeda, T. Motohiro, T. Sakai, H. Awano, R. Maekawa, Appl. Phys. Exp. **6**, 045501 (2013).
[8] M. Bouaziz, M. Amlouk, S. Belgacem, Thin Solid Films **517**, 2527 (2009).
[9] M. Nakashima, J. Fujimoto, T. Yamaguchi, M. Izaki, Appl. Phys. Exp. **8**, 042303 (2015).
[10] Y. Miyata, S. Nakamura, Y. Akaki, Phys. Status Solidi (c) **12**, 765 (2015).
[11] K. Chino, J. Koike, S. Eguchi, H. Araki, R. Nakamura, K. Jimbo, H. Katagiri, Jap. J. Appl. Phys. **51**, 10NC35 (2012).
[12] N. Aihara, H. Araki, A. Takeuchi, K. Jimbo, H. Katagiri, Phys. Status Solidi C **10,** 1086 (2013).
[13] Z. Tang, K. Kosaka, H. Uegaki, J. Chantana, Y. Nukui, D. Hironiwa, T. Minemoto, Phys. Status Solidi A **212**, 2289 (2015).
[14] P. A. Fernandes, P. M. P. Salom′e, A. F. da Cunha, J. Phys. D: Appl. Phys. **43**, 215403 (2010).
[15] H. Zhang, M. Xie, S. Zhang, Y. Xiang, J. Alloy. Compd. **602**, 199 (2014).
[16] D. M Berg, R. Djemour, L. G¨utay, G. Zoppi, S. Siebentritt, P. J. Dale, Thin Solid Films **520**, 6291 (2012).

[17] J. Koike, K. Chino, N. Aihara, H. Araki, R. Nakamura, K. Jimbo, H. Katagiri, Jap. J. Appl. Phys. **51**, 10NC34 (2012).

[18] M. Adelifard, M. M. Bagheri Mohagheghi, H. Eshghi, Phys. Scripta **85,** 035603 (2012).

[19] U. Chalapathi, Y. Jayasree, S. Uthanna, V. Sundara Raja, Phys. Status Solidi A **210,** 2384 (2013).

[20] Z. Su, K. Sun, Z. Han, F. Liu, Y. Lai, J. Li, Y. Liu, J. Mater. Chem. **22,** 16346 (2012).

[21] H. Dahman, S. Rabaoui, A. Alyamani, L. El Mir, Vacuum 101, 208 (2014).

[22] D. Tiwari, T. K. Chaudhuri, T. Shripathi, U. Deshpande, R. Rawat, Sol. Energy Mater. Sol. Cells **113**, 165 (2013).

[23] Z. Jia, Q. Chen, J. Chen, T. Wang, Z. Li, X. Dou, RSC Adv. **5**, 28885 (2015).

[24] D. M. Berg, R. Djemour, L. Gütay, S. Siebentritt, P. J. Dale, X. Fontane, V. Izquierdo-Roca, A. Pérez-Rodriguez, Appl. Phys. Lett. **100**, 192103 (2012).